Early-Stage Biosynthesis of Phenalinolactone Diterpenoids Involves Sequential Prenylation, Epoxidation, and Cyclization

Tyler A. Alsup[1], Zining Li[1], Caitlin A. McCadden[1], Annika Jagels[1,2], Diana Łomowska-Keehner[1], Erin Marshall[1,2], Liao-Bin Dong[3], Sandra Loesgen[1,2], Jeffrey D. Rudolf[1,*]

[1]Department of Chemistry, University of Florida, Gainesville, Florida, USA

[2]Whitney Laboratory for Marine Biosciences, University of Florida, St. Augustine, FL, United States

[3]State Key Laboratory of Natural Medicines, School of Traditional Chinese Pharmacy, China Pharmaceutical University, Nanjing 211198, Jiangsu, China

*To whom correspondence should be addressed: jrudolf@chem.ufl.edu

ABSTRACT

The chemical logic associated with assembly of many bacterial terpenoids remains poorly understood. We focused our efforts on the early-stage biosynthesis of the phenalinolactone diterpenoids, demonstrating that the *anti/anti/syn*-perhydrophenanthrene core is constructed by sequential prenylation, epoxidation, and cyclization. The functions and timing of PlaT1–PlaT4 were assigned by comprehensive heterologous reconstitution. We illustrated that the UbiA prenyltransferase PlaT3 acts on geranylgeranyl diphosphate (GGPP) in the first step of phenalinolactone biosynthesis, prior to epoxidation and cyclization. Finally, we isolated eight new-to-nature terpenoids, expanding the scope of the bacterial terpenome. The biosynthetic strategy employed in the assembly of the phenalinolactone core, with cyclization occurring after prenylation, is rare in bacteria and resembles fungal meroterpenoid biosynthesis. The findings presented here set the stage for future discovery, engineering, and enzymology efforts in bacterial meroterpenoids.

INTRODUCTION

Terpenoids are the largest family of natural products (NPs) with over 90,000 known members wielding a vast array of biological activities[1,2]. Their activities against bacteria, fungi, viruses, and cancer cell lines have driven natural products discovery efforts to identify novel terpenoids for applications in human health. Bacteria are commonly regarded as a trivial source of terpenoids; <2% of all known terpenoids are of bacterial origin[2]. However, there is a vast diversity of bacterial terpenoids and meroterpenoids and advances in genome sequencing and bioinformatics continue to reveal the immense biosynthetic potential encoded within bacterial genomes[3–5]. While terpenoid discoveries in bacteria are rapidly advancing in the genomic era, substantial knowledge gaps remain in how many of these complex small molecules are biosynthesized.

The phenalinolactones, diterpenoid glycosides isolated from *Streptomyces* sp. Tü 6071[6], are highly functionalized meroterpenoids with moderate antibacterial activities (Fig. 1A). The phenalinolactones bear an *anti*/*anti*/*syn*-perhydrophenanthrene core and several peripheral decorations including γ-butyrolactone,

L-amicetose and 5-methylpyrrole-2-carboxylic acid moieties[2,6]. Extensive work has been carried out to elucidate many of the late-stage tailoring and functionalization steps;[7–11] however, the biosynthesis of the diterpenoid scaffold, i.e., the perhydrophenanthrene core, remains elusive. Bioinformatic analysis of the *pla* BGC (Fig. 1B) led to an initial biosynthetic proposal (Fig. 1C). Geranylgeranyl diphosphate (GGPP), formed by the polyprenyl synthase PlaT4, is first epoxidized at the terminal alkene by the putative flavin-dependent monooxygenase, PlaT1, to yield 14,15-epoxy-GGPP[7]. The oxidosqualene cyclase-like (Fig. S1) type II terpene cyclase (TC)[12,13], PlaT2, was then proposed to catalyze cyclization via epoxide ring opening of epoxy-GGPP to afford the tricyclic core. The diphosphate moiety at C-15 of the cyclized product is presumed to be retained for the UbiA-like prenyltransferase, PlaT3, to subsequently add a three carbon α-keto acid;[7] the origin of this moiety is still unknown[7,8]. Inactivation of *plaT1*, *plaT2*, and *plaT3* in the native producer abolished production of the phenalinolactones and no intermediates were detected, supporting that these genes play crucial roles in formation of the diterpenoid core[7]. Since this initial proposal, similar hypotheses were made for the structurally related brasilicardins[14], tiancilactones[15], and atolypenes[16] (Fig 1A); each of these BGCs have homologs of PlaT1–PlaT4. The tetraterpenoid longestin (KS-505a) is also proposed to undergo the same three reactions, although a different timing was suggested[17,18]. There is currently no direct evidence for the functions of PlaT1–PlaT4, or their homologs, the timing in which they act, or their respective substrates and products.

Here, we report a revised proposal for the biosynthesis of the phenalinolactone diterpenoid core. Using heterologous expression, we (i) confirmed that the assembly of the diterpenoid core requires the four key enzymes PlaT1–PlaT4, (ii) demonstrated that prenylation by PlaT3 and epoxidation by PlaT1 occur prior to cyclization by PlaT2, and (iii) isolated eight novel phenalinolactone congeners. These findings support that each member of this family of bacterial terpenoids, as well as hundreds of their related BGCs[15], likely follow a similar biosynthetic strategy, but with distinct enzymes and modifications to achieve chemical diversity. This study also lays the foundation for investigating the mechanistic details of each of these enzymes.

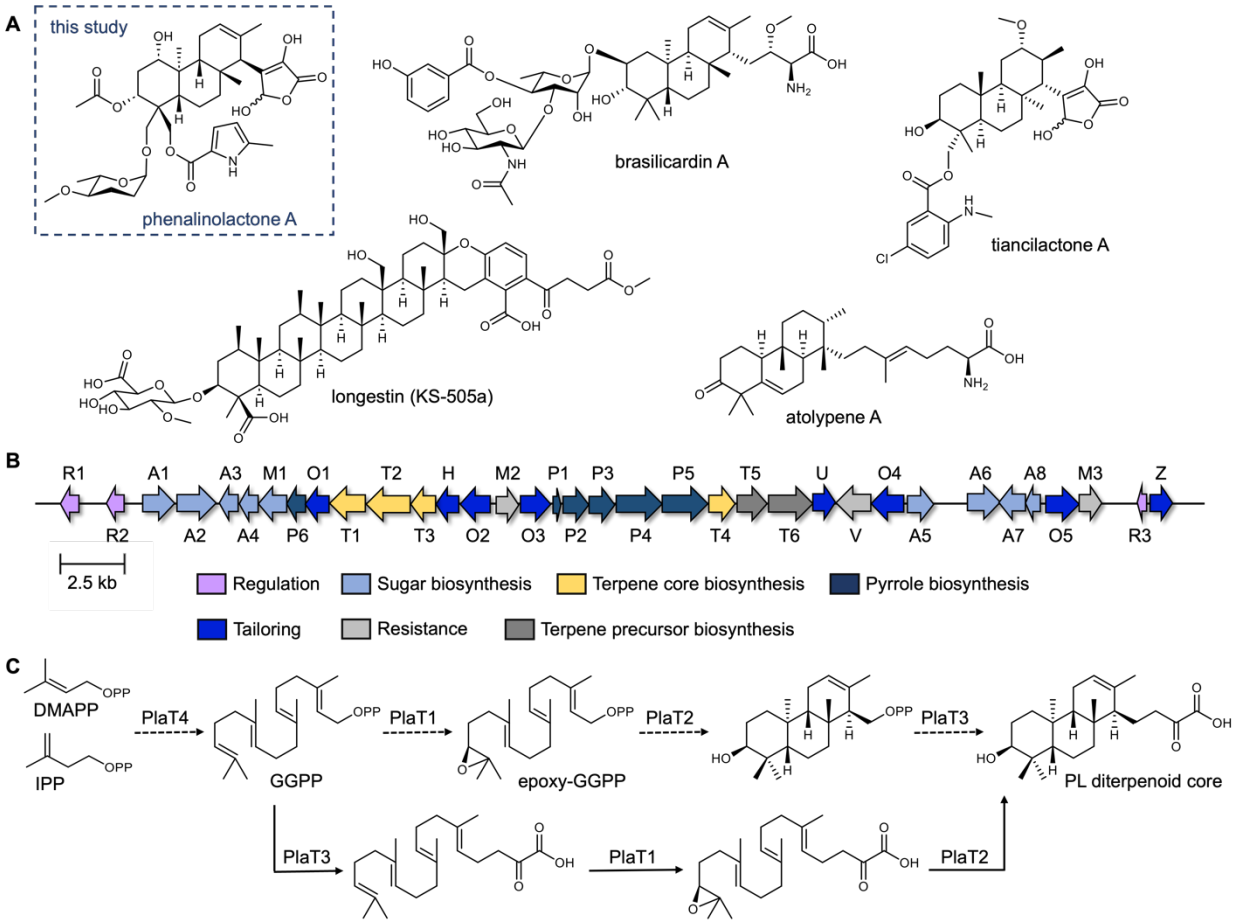

Figure 1. The phenalinolactone family of bacterial terpenoids and their proposed early-stage biosynthesis. (A) Phenalinolactone A and related terpenoids from bacteria[6,14–16,19]. (B) Phenalinolactone biosynthetic gene cluster (*pla*) from *Streptomyces* sp. Tü 6071. The roles, either confirmed or putative, of each gene are annotated according to the legend. The four core genes studied here, PlaT1–PlaT4, which are conserved throughout this family of terpenoids, are colored in yellow. (C) Previously proposed biosynthetic scheme suggesting the timing of PlaT1–PlaT4[7] (dashed lines) and biosynthetic scheme proposed in this study (solid lines).

RESULTS AND DISCUSSION

Formation of the diterpenoid core requires four enzymes

We first set out to determine if PlaT1–PlaT4 were required and sufficient for assembly of the diterpene scaffold. The four-gene cassette was reconstituted in the heterologous hosts *Streptomyces albus* J1074 and *Streptomyces venezuelae* under the control of the constitutive sp44 promoter (Figure S2)[20]. LC-MS analysis of the extracts revealed the production of two new metabolites **1** (*m*/*z* 374, $[M - H]^-$) and **2** (*m*/*z* 376, $[M - H]^-$) in *S. albus::plaT4321*; only **1** was produced in *S. venezuelae::plaT4321* (Figure 2A and 2B). Large-scale (18 L) fermentation of *S. albus::plaT4321* was carried out to isolate the metabolites for structural characterization. High-resolution ESIMS (HRESIMS) of **1** gave an $[M + H]^+$ ion at *m*/*z* 376.2852,

consistent with a molecular formula of $C_{23}H_{38}NO_3$ (calc. $[M + H]^+$ at 376.2851); **2** had a molecular formula of $C_{23}H_{40}NO_3$ based on an observed $[M + H]^+$ ion at *m/z* 378.3010 (calc. $[M + H]^+$ at 378.3008) (Figure S3). The structure of **1** was determined, by extensive 1D and 2D NMR spectroscopy (Table S4 and Figures S4–S9), to be a C_{23} tricyclic terpenoid bearing an amino acid tail and a ketone at C-3 (Figure 2C). The ^{13}C NMR data of **2** was almost identical to that of **1**, with the exception of the presence of a signal at 79.70 ppm instead of the ketone signal at 221.07 ppm (Table S5 and Figures S10–S15), supporting that **2** was the C-3 hydroxy analog of **1**. Oxidation of the hydroxyl of **2** to the ketone of **1** is plausibly carried out by a host oxidative enzyme and not the result of PlaT1–PlaT4. Key NOESY correlations of H-5/H-9, H-9/H_3-22, H_3-22/H_2-15, H-14/H_3-21 for both compounds supported their relative stereochemical assignments and the *anti*/*anti*/*syn* system of phenalinolactone A (Figures 2D, S9, and S15). The C-3 hydroxyl of **2** was supported as *S*-configured based on NOESY correlations between H-3/H_{ax}-2 and H-3/Me_{ax}-20 along with the correlations of H_{ax}-2/H_3-21, H_{eq}-1/-21, H-14/H_3-21. This assignment is consistent with the previous biosynthetic proposal that epimerization at the C-3 position, to the *R*-configured C-3 hydroxyl of PL CD6 (Fig. 2C), is catalyzed by an unidentified enzyme in the native producer enroute to the final natural product[7].

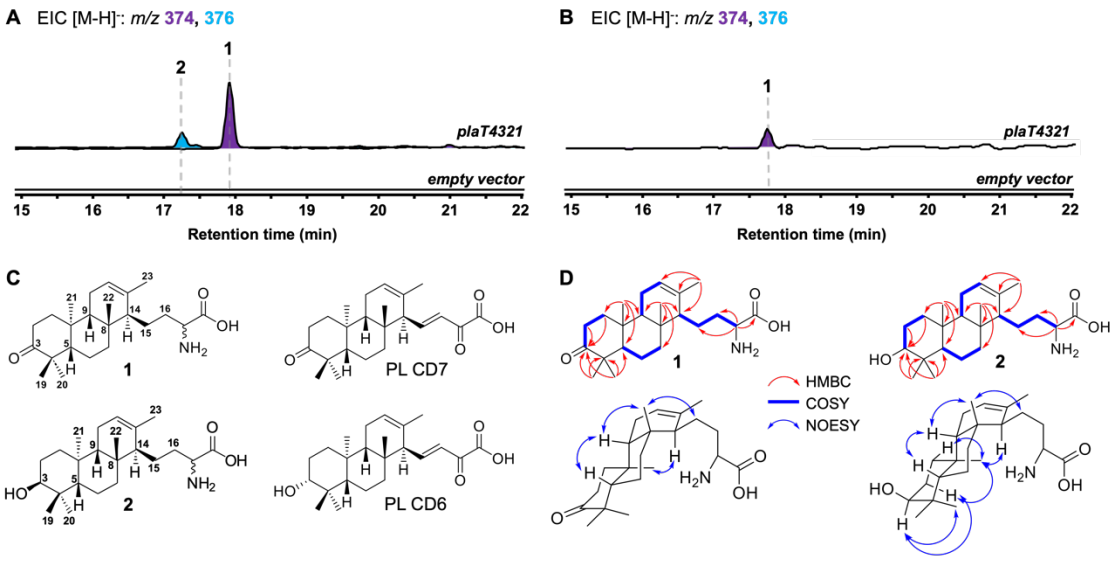

Figure 2. Reconstitution of the first four steps in phenalinolactone biosynthesis. (A and B) LCMS-EIC analysis of extracts obtained from *S. albus* (A) and *S. venezuelae* (B) hosts. (C) Cyclized diterpenoids (**1** and **2**) isolated in this study and previously isolated phenalinolactones PL CD6 and PL CD7 (ref. [7].) (D) Key HMBC, COSY, and NOESY correlations of **1** and **2**.

The tricyclic scaffolds of **1** and **2** are akin to those of the phenalinolactone intermediates PL CD6 and PL CD7, albeit with two key differences. Most notably, the amino acid moiety on **1** and **2** is different than the α-keto acid tail seen in PL CD6 and PL CD7 (Figure 2C). The presence of the amino acid moiety was surprising given that no phenalinolactones nor their known on-pathway intermediates, e.g., PL CD6 and PL CD7, possess this functional group. The tetronic acid moiety in the phenalinolactones is built from an α-

keto acid tail (Figure 1)[7]. The acyclic tail of **1** and **2**, however, resembles the immunosuppressive brasilicardins and the sesterterpenoid atolypenes (Figure 1A), whose BGCs both harbor aminotransferases that are proposed to convert the α-keto acid into the α-amino acid[16,21,22]. As no genes encoding an aminotransferase were included in the *plaT1–plaT4* construct, we surmised that the amino acid tails of **1** and **2** arise from an endogenous aminotransferase in the heterologous hosts. However, we cannot rule out that the prenyl acceptor in the UbiA reaction is an amino acid. Isolated products **1** and **2** also lack the double bond at C-15/C-16, thus none of the four PlaT1–PlaT4 enzymes are responsible for this oxidation. Furthermore, no related diterpenoids with this olefin were detected in either heterologous host indicating that they lack the proper machinery to perform this oxidation.

Epoxidation and prenylation precede cyclization

To determine the timing of the three key steps, epoxidation, prenylation, and cyclization, in the biosynthesis of the terpene core of phenalinolactone, we reconstituted combinations of *plaT1–plaT4* in *S. albus* and *S. venezuelae* (Figure S16). As anticipated, removing *plaT2* (i.e., *plaT431*), the gene encoding the terpene cyclase, abolished production of **1**, **2**, or any other tricyclic terpenoids in *S. albus::plaT431* and *S. venezuelae::plaT431* (Figure 3A and 3B). Instead, a number of new metabolites, **3**–**10**, with *m*/*z* ($[M - H]^-$) values ranging between 339 and 394 were detected in both strains. Metabolites **3**–**10** were observed in the extracts of *S. venezuelae::plaT431* while only **8**–**10** were seen in *S. albus::plaT431* (Figure 3A and 3B). A large-scale fermentation (18 L) of *S. venezuelae::plaT431* was carried out to isolate **3**–**7** for structural elucidation. Compounds **3**–**5** were determined to have 23, 22, and 20 carbons, respectively, based on HRESIMS and ^{13}C NMR analyses (Tables S6–S8, Figures S17–S32). The ^{13}C NMR spectra for **3**–**5** also revealed two signals between 70 and 80 ppm suggesting the presence of a pair of hydroxyl groups in each of the molecules. For **5**, key HMBC correlations of H_3-18 with C-10, C-11, and C-12, along with H-10 with C-9 and C-11 confirmed oxidation of the C-10/C-11 olefin; similar HMBC correlations were also observed for **3** and **4** (Figure 3C). HRESIMS and comprehensive NMR supported **3** to be an α-amino acid as observed in the tails of the cyclized terpenoids (**1** and **2**), whereas ^{13}C NMR resonances at 177.36 and 178.19 ppm, respectively, established **4** and **5** as carboxylic acids. Similarly, the molecular formulas of **6** ($C_{20}H_{36}O_5$) and **7** ($C_{22}H_{38}O_5$) were deduced by HRESIMS (Figure S33). The ^{13}C NMR spectra of **6** and **7** supported the presence of 20 and 22 carbons, respectively, with each showing four signals (70–90 ppm) for oxygenated carbons and a single signal consistent with the carboxylic acid seen in **4** and **5** (Tables S9 and S10, Figures S34–S43). A distinct spin system was observed in the ^1H-^1H COSY spectra of **6** (H_2-12/H_2-13/H-14) and **7** (H_2-14/H_2-15/H-16) and taken together with corroborative HMBC correlations, the presence of a tetrahydrofuran ring was determined (Figure 3C).

Compounds **8**–**10** had *m*/*z* values identical to **3**–**5** but with slightly different retention times (Figure 3A). A large-scale fermentation (18 L) of *S. albus::plaT431* was conducted to isolate **10**, which gave the chemical formula of $C_{20}H_{36}O_4$ by HRESIMS (Figure S44). The ^1H and ^{13}C NMR spectra of **10** were similar to that of

5, with a doublet methyl (δ_H 0.96 ppm) for C-20 and ^{13}C resonances at 73.34 ppm, 78.48 ppm, and 177.36 ppm, consistent with the diol and carboxylic acid functionalities in **5** (Table S11, Figures S45–S49). Analysis of the 2D NMR data of **10** confirmed the position of the diol at C-14/C-15, with key ^{1}H-^{13}C HMBC correlations of H_3-19 with C-14 and C-15 and H_3-20 with C-14 and C-15. The structures of **8** and **9** were proposed to be the C23 and C22 equivalents of **3** and **4**, respectively, based on HRESIMS (Figure S44) and comparisons of their retention times and relative yields to those of **3**–**5** (Figure 3). The presence of diols at C-10/C-11 of **5** (and the corresponding positions in **3** and **4**) and at C-14/C-15 in **10** suggests epoxidation of either an internal or terminal alkene of the prenyl tail. The terminal position is required for the biosynthesis of **1** and **2** via cyclization by PlaT2. The presence of C23 (**3** and **8**), C22 (**4**, **7**, and **9**), and C20 (**5**, **6**, and **10**) oxidized metabolites hints towards oxidative degradation of the carboxylic acid end of the metabolites, similar to what was previously seen for bacterial isoprenoid and fatty acid degradation (Figure S50).[23,24]

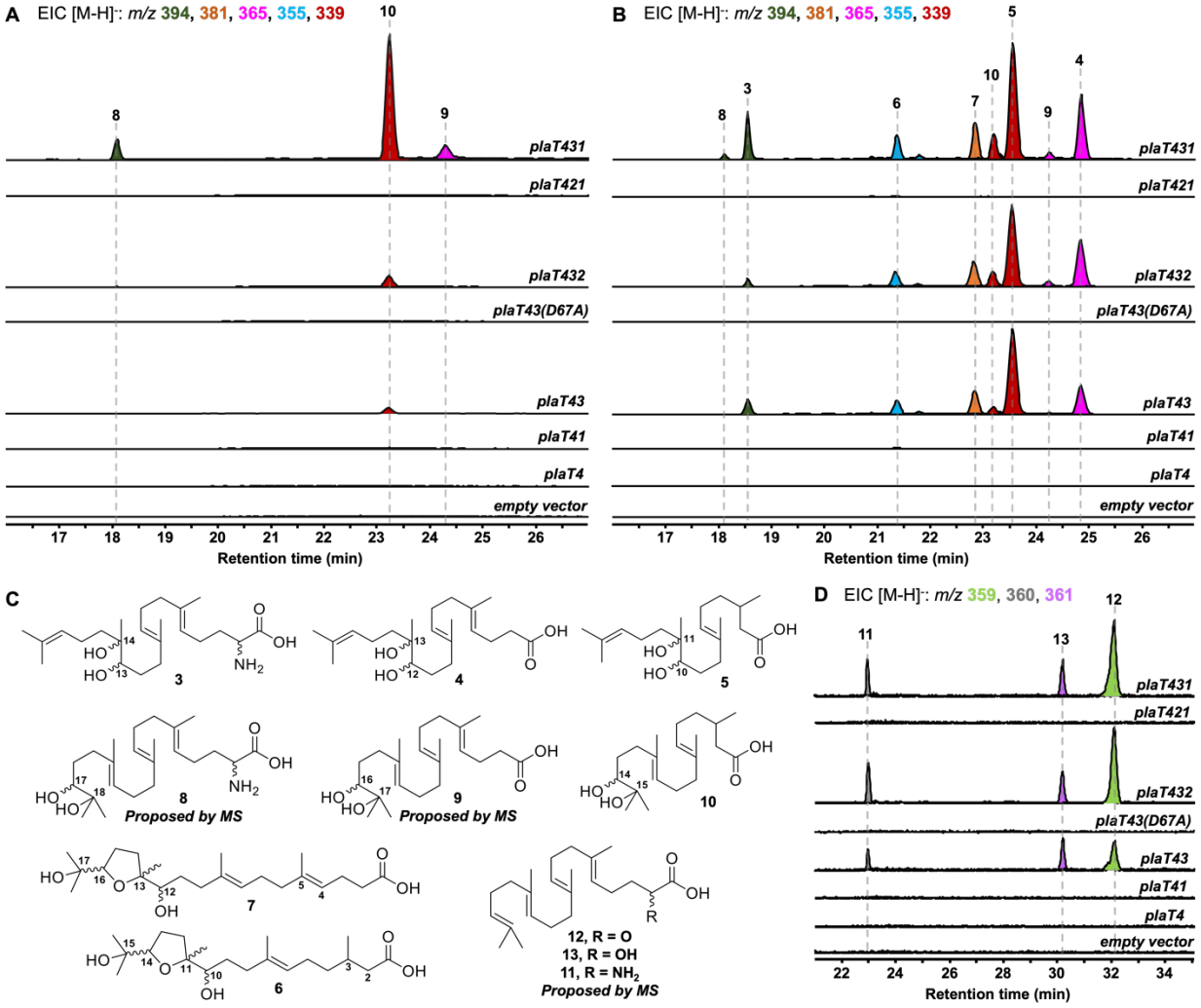

Figure 3. Reconstitution of various combinations of genes involved in biosynthesis of the phenalinolactone diterpenoid core. LCMS-EIC analysis of extracts obtained from *S. albus* (A and D) and *S. venezuelae* (B) hosts. (C) Isolated and structurally determined terpenoid metabolites.

Prenylation by PlaT3 is the first step in phenalinolactone biosynthesis

We next set out to determine the order of epoxidation and prenylation by PlaT1 and PlaT3, respectively. LC-MS analysis of our *pla* constructs revealed that *plaT3* is required for production of **3**–**10**. Hosts expressing *plaT43*, *plaT432*, or *plaT431* produced several diterpenoids, whereas hosts expressing *plaT4*, *plaT41*, or *plaT421*, i.e., those without *plaT3*, did not produce any detectable diterpenoids (Figure 3A and 3B). The presence of several oxidized terpenoids seen in hosts expressing *plaT43* (or *plaT432*), when no oxidase was included, complicated our study of the timing of epoxidation and prenylation. Oxidation was seen at two different positions, the middle alkene (**3**–**5**), terminal alkene (**8**–**10**), or both (**6** and **7**; Fig. S51), particularly in *S. venezuelae* and even in the absence of *plaT1*. We suspected that an endogenous enzyme(s) in the host *Streptomyces* was oxidizing the C23 prenylated intermediate. This idea was supported by the presence of **3**–**7** only in *S. venezuelae*, which must have an endogenous enzyme that oxidizes the internal alkene but is absent in *S. albus*. However, we could not rule out these oxidations were occurring prior to prenylation. Thus, we generated the construct *plaT43*(*D67A)*, which contained a mutation in PlaT3 rendering it inactive, to ensure that PlaT3 was not acting as an oxidase and to support that its prenylation activity was required to produce **3**–**10**. We targeted an Asp residue that was previously shown to be essential for catalyzing prenylation in characterized UbiA family prenyltransferases[25,26]. Gratifyingly, the expression of *plaT43*(*D67A)* in both hosts did not yield any of the metabolites **3**–**10** (Figure 3A and 3B).

Further examination of the LC-MS data from *S. albus* hosts harboring *plaT3* uncovered three additional metabolites, **11**–**13**, with *m/z* ($[M - H]^-$) values of 359, 361, and 360, respectively (Figure 3D). Unfortunately, very low yields of these metabolites in large-scale fermentation prevented isolation and structure elucidation by NMR. However, HRESIMS gave an $[M - H]^-$ value of *m/z* 360.2907 (calc. $[M - H]^-$ at 360.2903) for **11**, indicating a molecular formula of $C_{23}H_{39}NO_2$ (Figure S52). Consistent with the production of **3**–**10**, metabolites **11**–**13** were not produced in any constructs lacking *plaT3* or the inactive mutant *plaT43*(*D67A)* (Figure 3D). The presence of **11**–**13** further supports that prenylation occurs prior to both oxidation and cyclization, implicating that PlaT3 acts on GGPP in the first step of phenalinolactone biosynthesis (Figure 4). Since the active sites of functionally characterized UbiA prenyltransferases accommodate the diphosphate of a prenyl donor and a small, often aromatic, prenyl acceptor, it is logical that PlaT3 catalyzes the condensation of GGPP and a three-carbon α-keto acid prenyl acceptor[25–27]. Overall, an updated proposal for the early-stage biosynthesis of the phenalinolactones involves sequential prenylation by PlaT3, epoxidation by PlaT1, and cyclization by PlaT2 (Figure 4).

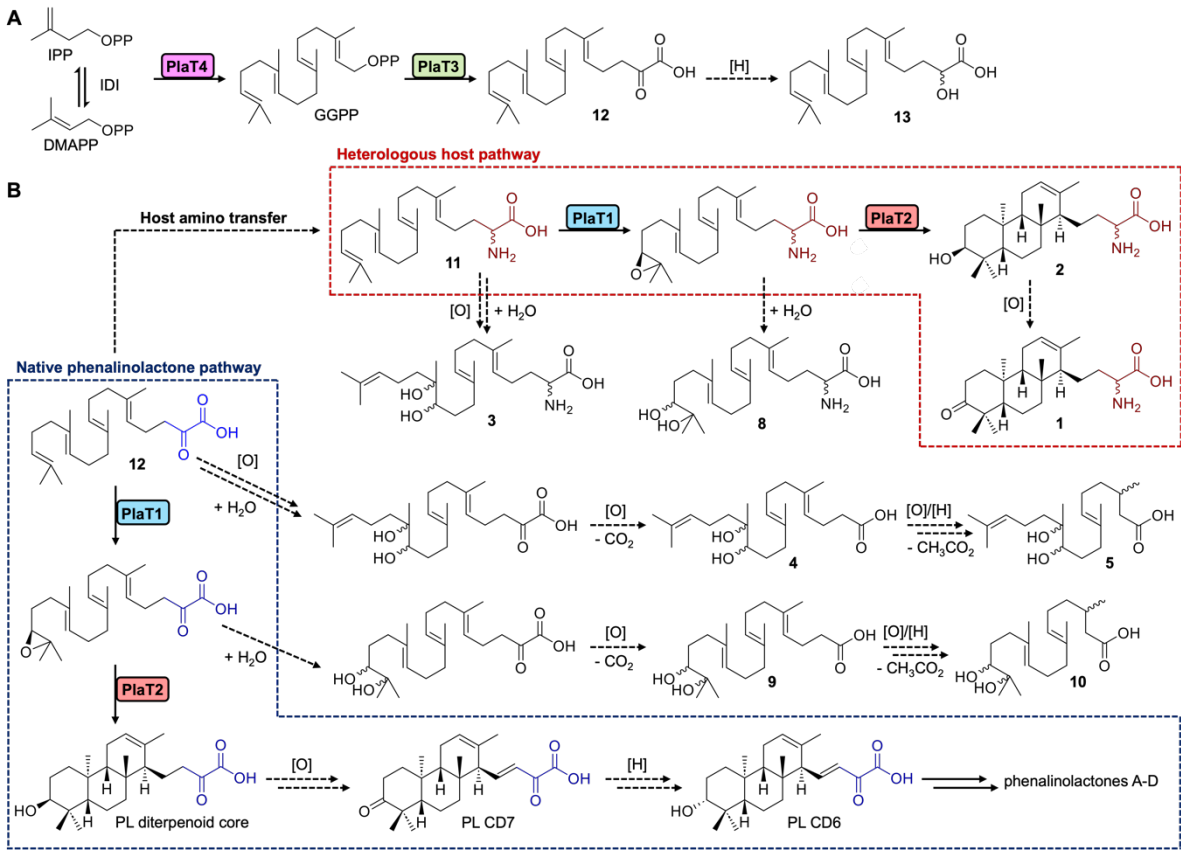

Figure 4. Proposed pathway for the biosynthesis of the phenalinolactone diterpenoid core.

(A) Proposed biosynthesis of prenylated intermediates **12** and **13** from IPP and DMAPP. (B) Proposed biosynthetic scheme from the common intermediate **12** for amino acid and keto acid pathways. Dashed arrows labeled only with [H] or [O] denote off-pathway enzymatic reduction or oxidation steps in the heterologous hosts, or undetermined enzymatic steps in the native producer (towards PL CD7 and PL CD6). In the heterologous hosts amino transfer may also occur after oxidation (**3** and **8**) or cyclization (**1** and **2**).

CONCLUSIONS

Bacteria represent a treasure trove of biosynthetic potential. While genomic data has driven a reinvigorated effort in the discovery of novel natural products, many biosynthetic pathways have yet to be fully elucidated. By employing heterologous expression, we uncovered new insights into early-stage biosynthesis of the phenalinolactone diterpenoids, demonstrating that assembly of the *anti/anti/syn*-perhydrophenanthrene core is accomplished via sequential prenylation, epoxidation, and cyclization. These findings are in stark contrast to the previously proposed pathway, where PlaT1 was thought to epoxidize GGPP prior to prenylation by PlaT3. Epoxidation of prenyl diphosphates has not been previously observed in terpenoid pathways; epoxidation typically occurs on substrates lacking the diphosphate group (e.g., squalene or prenylated meroterpenoids). In fact, modification of prenyl diphosphates is rare, with only methylation and

hydroxylation known[28,29]. Structurally and mechanistically, PlaT2 is akin to oxidosqualene cyclases (OSCs) involved in steroid biosynthesis. Both OSC and PlaT2 accommodate an epoxy substrate lacking the diphosphate head group and initiate cyclization via protonation of the epoxide ring to yield terpenoid scaffolds with C-3 hydroxy functionalities. Interestingly, early-stage biosynthesis of the phenalinolactones follows a similar biosynthetic logic as often described in fungal meroterpenoid pathways (Figure S53), where prenylation and epoxidation occur prior to cyclization. Overall, we propose that the phenalinolactones and related family members (i.e. brasilicardins, tiancilactones, and atolypenes) likely follow a shared biosynthetic rationale, although definitive evidence via in vitro data is still required to confirm that possibility. In parallel to this study, an analogous biosynthetic investigation was performed on the atolypene sesterterpenoids, indicating that prenylation and epoxidation also precede cyclization in *ato* biosynthesis.[30] However, the timing of prenylation and epoxidation in the atolypenes may be different. No products were seen in the construct containing the *ato* polyprenyl synthase (AtoC) and UbiA prenyltransferase (AtoD) and a hydrolyzed derivative of 14,15-epoxygeranylgeraniol was isolated from a construct without AtoD.[30] In conclusion, our findings underline Nature's highly evolved strategies for terpenoid scaffold assembly, providing new insights into terpene biochemistry and establishing the foundation for future discovery, engineering, and enzymology efforts. We envision that a thorough biosynthetic understanding of this family of bacterial terpenoids will help to guide genome mining of novel natural products and facilitate engineering of enzymes and pathways for the production of bioactive metabolites.

EXPERIMENTAL PROCEDURES

All experimental procedures are described in detail in the supplemental information.

Resource availability

Further information and requests for resources should be directed to and will be fulfilled by the lead contact, Jeffrey D. Rudolf (jrudolf@chem.ufl.edu).

Materials availability

Plasmids generated in this study will be made available on request. All other materials are commercially available or can be prepared as indicated.

Data and code availability

All data are included in the main text and supplemental information.

SUPPLEMENTAL INFORMATION

Supplemental information can be found online.

ACKNOWLEDGMENTS

This work was funded in part by NIH Grants R00 GM124461 and R35 GM142574 (to J.D.R.) and NSF Grant CHE-2020110 (to S.L.). T.A.A. was supported in part by an NIH Chemistry-Biology Interface Research Training Program Grant T32 GM136583. We acknowledge the University of Florida Mass

Spectrometry Research and Education Center (MSREC), which is supported by the NIH (S10 OD021758-01A1). We acknowledge both the University of Florida Center for Nuclear Magnetic Resonance Spectroscopy and the University of Florida McKnight Brain Institute at the National High Magnetic Field Laboratory's Advanced Magnetic Resonance Imaging and Spectroscopy (AMRIS) Facility, which is supported by the US NSF Cooperative Agreement No. DMR-1644779 and the State of Florida, for NMR support. We would like to give special thanks to Drs. James Rocca and Ion Ghiviriga for their incredible NMR support. Finally, we thank Prof. Dr. Axel Zeeck for generously gifting *Streptomyces* sp. Tü 6071.

AUTHOR CONTRIBUTIONS

Conceptualization, J.D.R.; methodology, T.A.A. and J.D.R.; investigation, T.A.A., Z.L., C.A.M., A.J., D.Ł.K., and E.M.; data analysis, T.A.A., Z.L., C.A.M., A.J., D.Ł.K., E.M., L.-B.D., S.L., and J.D.R.; writing – original draft, T.A.A. and J.D.R.; writing – review & editing, T.A.A., Z.L., C.A.M., A.J., D.Ł.K., E.M., L.-B.D., S.L., and J.D.R.; visualization, T.A.A. and J.D.R.; supervision, J.D.R.; funding acquisition, S. L. and J.D.R.

DECLARATION OF INTERESTS

The authors declare no competing interests.

REFERENCES

1. *Dictionary of Natural Products*, http://dnp.chemnetbase.com (accessed Mar 19, 2024).
2. J. D. Rudolf, T. A. Alsup, B. Xu and Z. Li, *Nat. Prod. Rep.*, 2021, **38**, 905 – 980.
3. D. E. Cane and H. Ikeda, *Acc. Chem. Res.*, 2012, **45** (3), 463 – 472.
4. M. Nett, H. Ikeda and B. S. Moore, *Nat. Prod. Rep.*, 2009, **26**, 1362 – 1384.
5. Y. Yamada, T. Kuzuyama, M. Komatsu, K. Shin-ya, S. Omura, D. E. Cane and H. Ikeda, *Proc. Natl. Acad. Sci.*, 2014, **112** (3), 857 – 862.
6. K. Gebhardt, S. W. Meyer, J. Schinko, G. Bringmann, A. Zeeck and H.-P. Fiedler, *J. Antibiot.*, 2011, **64** (3), 229 – 232.
7. C. Dürr, H.-J. Schnell, A. Luzhetskyy, R. Murillo, M. Weber, K. Welzel, A. Vente and A. Bechthold, *Chem. Biol.*, 2006, **13** (4), 365 – 377.
8. M. Daum, H.-J. Schnell, S. Herrmann, A. Günther, R. Murillo, R. Müller, P. Bisel, M. Müller and A. Bechthold, *Chembiochem*, 2010, **11** (10), 1383 – 1391.
9. T. Binz, S. C. Wenzel, H.-J. Schnell, A. Bechthold and R. Müller, *Chembiochem*, 2008, **9** (3), 447 – 454.
10. C. Kiske, A. Erxleben, X. Lucas, L. Willmann, D. Klementz, S. Günther, W. Römer and B. Kammerer, *Rapid Commun. Mass Spectrom.*, 2014, **28** (13), 1459 – 1467.

11. M. Myronovskyi, E. Welle, V. Fedorenko and A. Luzhetskyy, *Appl. Environ. Microbiol.*, 2011, **77** (15), 5370 – 5383.

12. D. W. Christianson, *Chem. Rev.*, 2017, **117** (17), 11570 – 11648.

13. X. Pan, J. D. Rudolf and L.-B. Dong, *Nat. Prod. Rep.*, 2024, Advance Article.

14. H. Shigemori, H. Komaki, K. Yazawa, Y. Mikami, A. Nemoto, Y. Tanaka, T. Sasaki, Y. In, T. Ishida and J. Kobayashi, *J. Org. Chem.*, 1998, **63** (20), 6900 – 6904.

15. L.-B. Dong, J. D. Rudolf, M.-R. Deng, X. Yan and B. Shen, *Chembiochem*, 2018, **19**, 1727.

16. S.-W. Kim, W. Lu, M. K. Ahmadi, D. Montiel, M. A. Ternei and S. F. Brady, *ACS Synth. Biol.*, 2019, **8** (1), 109 – 118.

17. S. Nakanishi, K. Osawa, Y. Saito, I. Kawamoto, K. Kuroda and H. Kase, *J. Antibiot.*, 1992, **45** (3), 341 – 347.

18. T. Ozaki, S. S. Shinde, L. Gao, R. Okuizumi, C. Liu, Y. Ogasawara, X. Lei, T. Dairi, A. Minami and H. Oikawa, *Angew. Chem. Int. Ed. Engl.*, 2018, **57** (22), 6629 – 6632.

19. F. Wei, W. Li, R. Song and Y. Shen, *Nat. Prod. Commun.*, 2018, **13** (11), 1433 – 1436.

20. S. J. Moore, H.-E. Lai, S.-M. Chee, M. Toh, S. Coode, K. Chengan, P. Capel, C. Corre, E. L. C. de los Santos and P. S. Freemont, *ACS Synth. Biol.*, 2021, **10** (2), 402 – 411.

21. A. Botas, M. Eitel, P. N. Schwarz, A. Buchmann, P. Costales, L. E. Núñez, J. Cortés, F. Morís, M. Krawiec, M. Wolański, B. Gust, M. Rodriguez, W.-N. Fischer, B. Jandeleit, J. Zakrzewska-Czerwińska, W. Wohlleben, E. Stegmann, P. Koch, C. Méndez and H. Gross, *Angew. Che. Intl. Ed. Engl.*, 2021, **60** (24), 13536 – 13541.

22. P. N. Schwarz, A. Buchmann, L. Roller, A. Kulik, H. Gross, W. Wohlleben and E. Stegmann, *Biotechnol. J.*, 2018, **13** (2), 1700527.

23. W. Seubert, *J. Bacteriol.*, 1960, **79** (3), 426 – 434.

24. K. Rose and A. Steinbüchei, *Appl. Environ. Microbiol.*, 2005, **71** (6).

25. S. Ren, N. A. W. de Kok, Y. Gu, W. Yan, Q. Sun, Y. Chen, J. He, L. Tian, R. L. H. Andringa, X. Zhu, M. Tang, S. Qi, H. Xu, H. Ren, X. Fu, A. J. Minnaard, S. Yang, W. Zhang, W. Li, Y. Wei, A. J. M. Driessen and W. Cheng, *Cell Rep.*, 2020, **33** (3), 108294.

26. H. Huang, E. J. Levin, S. Liu, Y. Bai, S. W. Lockless and M. Zhou, *PLOS Biol.*, 2014, **12** (7), 1001911.

27. K. Zhang, G. Zhang, X. Hou, C. Ma, J. Liu, Q. Che, T. Zhu and D. Li, *Org. Lett.*, 2022, **24** (10), 2025 – 2029.

28. C. Ignea, M. H. Raadam, A. Koutsaviti, Y. Zhao, Y.-T. Duan, M. Harizani, K. Miettinen, P. Georgantea, M. Rosenfeldt, S. E. Viejo-Ledesma, M. A. Petersen, W. L. P. Bredie, D. Staerk, V. Roussis, E. Ioannou and S. C. Kampranis, *Nat. Commun.*, 2022, **13**, 5188.

29. H. Tsutsumi, Y. Katsuyama, M. Izumikawa, M. Takagi, M. Fujie, N. Satoh, K. Shin-ya, and Y. Ohnishi, *J. Am. Chem. Soc.*, 2018, **140** (21), 6631 – 6639.

30. Z. Wang, T. A. Alsup, X. Pan, L. Li, J. Tian, Z. Yang, X. Lin, H.-M. Xu, J. D. Rudolf, and L.-B. Dong. Unpublished, submitted to *ChemRxiv*.